Lab on a Chip

RSC Publishing

CRITICAL REVIEW

View Article Online
View Journal | View Issue

Microfabricated mammalian organ systems and their integration into models of whole animals and humans

Cite this: *Lab Chip*, 2013, **13**, 1201

Jong H. Sung,[a] Mandy B. Esch,[b] Jean-Matthieu Prot,[b] Christopher J. Long,[c] Alec Smith,[c] James J. Hickman[cd] and Michael L. Shuler*[b]

While *in vitro* cell based systems have been an invaluable tool in biology, they often suffer from a lack of physiological relevance. The discrepancy between the *in vitro* and *in vivo* systems has been a bottleneck in drug development process and biological sciences. The recent progress in microtechnology has enabled manipulation of cellular environment at a physiologically relevant length scale, which has led to the development of novel *in vitro* organ systems, often termed 'organ-on-a-chip' systems. By mimicking the cellular environment of *in vivo* tissues, various organ-on-a-chip systems have been reported to reproduce target organ functions better than conventional *in vitro* model systems. Ultimately, these organ-on-a-chip systems will converge into multi-organ 'body-on-a-chip' systems composed of functional tissues that reproduce the dynamics of the whole-body response. Such microscale *in vitro* systems will open up new possibilities in medical science and in the pharmaceutical industry.

Received 6th September 2012,
Accepted 9th January 2013

DOI: 10.1039/c3lc41017j

www.rsc.org/loc

1 Introduction

In vitro models of human tissues are invaluable tools for research and drug discovery. Experimentation with *in vitro* models that mimic the *in vivo* metabolism and respond to stimuli authentically, *i.e.* that behave similar to those *in vivo*, provide the most meaningful results. While some tissue models are well established and used successfully for selected aspects of drug screening (for example the Caco-2 model of the GI-tract epithelium[1]), other tissues such as the blood brain barrier are more difficult to re-create. It has been shown that the microenvironments in which cells grow play an essential role in providing important mechanical and chemical cues that are needed to promote authentic cellular behavior.[2]

In recent years, the use of microtechnology has become an indispensable strategy to manipulate cell growth environments. The size scale at which microtechnology operates is highly relevant to living tissues. For example, the most commonly fabricated devices are microfluidic channels of sizes between 10–200 μm. In comparison, mammalian cells are 8–30 μm in size, and the diameters of microvascular capillaries range from 10–500 μm. Adaptation of the microtechnology in the semiconductor industry to the field of tissue engineering resulted in various novel technologies, such as microfluidic cell patterning and manipulation,[3] hydrogel microfabrication,[4] and serum-free media formulation for multiple cell types.[5–7] These techniques have allowed researchers to place a variety of cell types in physiologically realistic proximity to each other and thereby create multi-cell type tissue constructs as well as tissue-tissue boundaries.[8] The stiffness of the substrate and shear stresses exerted on the cells can be controlled to match the physiological levels. Furthermore, fluid-to-cell ratios within microfluidic devices are much closer to physiological levels than in conventional cell culture dishes. Drug concentrations and fluid residence times can be more accurately mimicked using microfabricated cell growth reactors.

This review will discuss a variety of *in vitro* microscale tissue models, and describe how these single tissue models can be integrated into multi-tissue devices, often termed 'body-on-a-chip' or 'human-on-a-chip' devices.[9,10] One of the most important advantages of microtechnology in terms of body-on-a-chip devices is that the tissue chambers can be connected by a set of microfluidic channels mimicking blood vessels. Testing new drugs for toxic side effects or activated compounds as a result of liver metabolism is one of the most important considerations in drug development.[11] Body-on-a-chip cell culture platforms can simulate tissue-tissue interactions in a more physiologically realistic manner, improving the efficiency of drug development process.

[a]*Chemical Engineering, Hongik University, Seoul, Korea*
[b]*Biomedical Engineering, Cornell University, USA. E-mail: mls50@cornell.edu; Tel: 607 255-7577*
[c]*Nanoscience Technology Center, University of Central Florida, USA*
[d]*Biomolecular Science Center, Burnett School of Biomedical Sciences, University of Central Florida, USA*

2 Microfabricated organ models

Microfabrication technology has been applied to mimic various organ systems. Novel strategies have therefore been

developed to reproduce certain aspects of the necessary tissue environment *in vitro*. *In vivo* tissue traits recreated *in vitro* so far include tissue geometries,[12] cell compositions,[13] biomolecular gradient,[14] and mechanical movement.[15] In this section, we describe how microfabrication strategies have been applied to the development of accurate representation of *in vivo* organs and how they led to more authentic *in vitro* organ functionalities.

2.1 Microvasculature

Microfluidics, dealing with extremely small quantities of liquid in microscale channels, is an ideal technology for recreating the microenvironment of the vasculature. Several factors are involved in the microenvironment of the blood vessels, including fluidic shear stress, peristaltic movement, chemical gradient, and cell to cell communication. The low Reynolds number typically achieved in a microfluidic system enables precise control of these factors, allowing researchers to study the combinatorial effect of the factors.

The fluid dynamics and transport phenomena inside microfluidic systems can be analyzed theoretically. In simple cases an analytical solution may be obtained but it is more typical to use a computational method. The flow inside a microfluidic channel can be analyzed by solving Navier–Stokes equation, assuming incompressible fluid:

$$\rho\frac{\partial\vec{u}}{\partial t} = -\rho\vec{u}\nabla\vec{u} - \nabla p + \eta\nabla^2\vec{u} \quad (1)$$

(Rate of change of momentum) = (Convective force) + (Pressure force) + (Viscous force)

Where u is the velocity field (m s^{-1}), ρ is the density (kg m^{-3}), η is the viscosity (Pa s), p is the pressure (Pa). In the simple case of a long, cylindrical tube with the radius R, the steady-state flow rate can be described by following equation.

$$Q = \frac{\pi R^4}{8\eta}\left(-\frac{dp}{dx}\right) = \frac{\pi R^4}{8\eta}\frac{\Delta p}{L} \quad (2)$$

Where Δp is the pressure drop across the channel with the length of L and η is viscosity (Pa s). The eqn (2) relates the volumetric flow rate with the pressure drop and the geometry of the channel (the radius and the length). An analogy to an electrical circuit can be made by relating the flow rate (Q) to the current (I), and the pressure drop (Δp) to the voltage drop (ΔV), then an equation similar to the Ohm's law can be written.

$$\Delta V = IR \text{ (electrical wire)}, \quad \Delta p = QR \text{ (fluidic channel)} \quad (3)$$

In fluid dynamics, the resistance R is dictated mainly by the geometry of the channel. In the case of a rectangular channel with a high aspect ratio ($w \gg h$), the resistance can be described by the following equation:

$$R = \frac{12\mu L}{wh^3} \quad (4)$$

Analogy of a microfluidic system with an electrical circuit allows a network of microfluidic channels to be analyzed in a similar manner.[16,17] For example, the fluidic resistance of serially connected microfluidic channels is the same as the sum of fluidic resistance of all channels. In a similar manner, the reciprocal of the fluidic resistance of parallel-connected microfluidic channels is the same as the sum of the reciprocal of the resistance of all channels.

Microfluidic systems allow researchers to precisely control the parameters that define the microenvironment of *in vivo* tissues, enabling parametric study of the relationship between environment and cellular behavior. Young *et al.* used a microfluidic device to study the adhesion properties of endothelial cells in the presence of various extracellular matrix (ECM) proteins and fluidic shear stresses.[18] The fluidic shear stress in a parallel plate is determined by the geometry of the channel and the fluid velocity in the following manner:

$$\tau = \frac{6\mu Q}{wh^2} \quad (5)$$

where μ is the viscosity, Q is the flow rate, w is the width and h is the height of the channel. A unique advantage of using microfluidics was demonstrated in a study that used a microscale channel with a tapered profile, generating a wide range of shear stresses.[19] It is noteworthy that in many studies, a combinatorial effect of various environmental factors on cell behavior was studied, for example ECM proteins and shear stress,[18] signaling molecules and shear stress.[20,21]

While polydimethylsiloxane (PDMS) is the most popular material for microfluidic systems and carries many advantages, the material properties of the PDMS surface are not biologically relevant.[22] On the other hand, ECM proteins or hydrogels provide scaffolds that resemble the natural *in vivo* tissue environment better than PDMS.[23] Also hydrogels are more porous than PDMS, allowing molecular diffusion inside the hydrogel scaffold.[24] Therefore, many efforts have been directed toward fabricating hydrogel into a microfluidic scaffold.[25,26] Other hydrogels have been used to create microfluidic devices, such as polyethylene glycol diacrylate (PEG-DA),[27] and fibrin.[28] While these approaches focused on creating a rather simple representation of the blood vasculature, a different approach focused on recreating a more complex vasculature network. A sacrificial molding technique was used to create an interconnected network inside a scaffold made of collagen[28] or PDMS.[29]

2.2 Lung and gas transfer

In the lung, the interface between air in the alveoli and blood in the surrounding capillaries is characterized by a bilayer of alveolar epithelial cells and microvascular endothelial cells, as well as surfactant and mucus produced by specialized cells in the epithelium. This interface acts primarily to deliver oxygen to and remove carbon dioxide from the blood, but also acts as a physical barrier to inhaled insults.[30] The microenvironment

for the epithelial–endothelial bilayer includes an air–liquid interface with appropriate partial pressures and dissolved gas concentrations and mechanical stretching resulting from the action of breathing. Several microdevices have been designed to recreate portions of the lung physiology. The physiological epithelial monolayer using an air–liquid interface has been developed.[31] This air–liquid interface was shown to influence the integrity of the epithelial layer and to increase the production of surfactant, similar to the native epithelium in the lung. A microfluidic device was used to model the airway architecture to simulate abnormal obstruction of small airways and to study the effect of liquid plug propagation and rupture on the alveolar epithelial cells lining the alveoli.[32] The addition of a surfactant significantly reduced damage to the epithelium, providing evidence that such a device may be useful for evaluating methods for reducing airway damage due to occlusion and clearing of small airways. The addition of mechanical stretch to a device with similar fluid-based airway obstruction produced a device that combined physiological solid mechanical stresses with fluid stresses on alveolar epithelial cells.[33]

Recently, a PDMS system that incorporated both an air-facing epithelial cell monolayer and a liquid-facing endothelial cell monolayer of the alveolar-capillary air–liquid interface was produced.[15] The two layer device was designed to allow controlled mechanical stretching of the endothelial–epithelial bilayer, mimicking the mechanical cues present in the lung during breathing. When mechanical stretching was applied to the bilayer system under flow, organ-level responses to bacteria, adhesion of neutrophils, and pathogen phagocytosis were recreated. The extremely high gas permeability of PDMS commonly used for these types of devices limits the on-device control and measurement of the gas concentrations in the media and air phases on the device, both of which are important for recreating the microenvironment of the alveoli. Iterative computational fluid dynamics and experimental flow visualization were used to design microfluidic paths and internal structures to control the liquid side flow in a silicon-based device (Fig. 1(A)).[34]

2.3 Liver metabolism and *in vitro* metabolism

The first-pass metabolism refers to the metabolism of a drug during oral absorption. Before a drug reaches the systemic circulation, it goes through the intestine and the liver, where it is metabolized by intestinal enzymes, microbial enzymes, and hepatic enzymes. The liver is strategically located behind the gastrointestinal (GI) tract to detoxify xenobiotics, and receives blood from the GI tract through the portal vein. Since it has as profound effect on the final effect of a drug, reproducing the liver metabolism *in vitro* has been of great interest. The liver

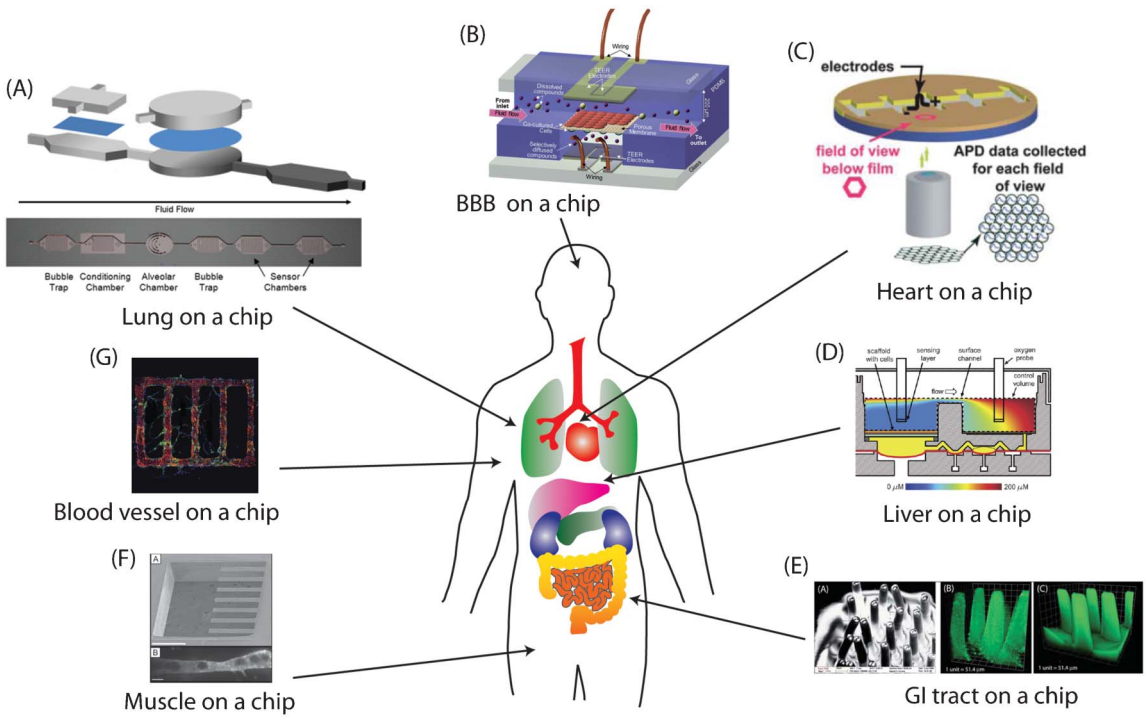

Fig. 1 Microfabricated organ systems mimicking various organ tissues. (A) Lung on a chip device modeling an alveolus and layout of fluid side of lung-based body-on-a-chip device fabricated in silicon. Reprinted from Long *et al.*[34] with permission from Springer. (B) BBB on a chip, consisting of two perpendicular channels separated by a membrane. Reprinted with permission from Booth *et al.*[60] (C) The contractility of heart tissue is measured using the muscular thin film (MTF). Reprinted with permission from Grosberg *et al.*[79] (D) A microfluidic bioreactor for 3D liver tissue engineering. Reprinted with permission from Domansky *et al.*[40] (E) Microscale hydrogel scaffold mimicking the intestinal villi geometry. Reprinted with permission from Sung *et al.*[41] (F) Cantilever for detecting myotube contraction. Above: SEM micrograph of silicon cantilever array at 60× magnification. (scale bar = 5004 m), Below: Confocal micrograph detailing top down view of a single cultured myotube on a cantilever. (scale bar = 204 m). Reproduced with permission from Wilson *et al.*[86] (G) Microvascular network in 3D tissue scaffold made of collagen matrix. Reprinted with permission from Zheng *et al.*[26]

metabolism can be divided into two types of reactions; phase I and phase II metabolism. The phase I metabolism includes hydrolysis, oxidation, and reduction reactions while the phase II metabolism mainly consists of conjugation reactions.[35] Cytochrome P450 enzymes play dominant roles in the phase I reaction, while various enzymes such as uridine diphosphoglucuronosyl transferase (UGT), glutathione S-transferase (GST), and sulfotransferase (ST) are involved in the phase II reactions.

Various *in vitro* systems for reproducing the liver metabolism have been developed. While liver slices[36] or primary hepatocytes[37] are considered to demonstrate metabolic profiles similar to the liver over a short period of time, the scarcity of the model system and the difficulty with using the system hinders them from being widely used models, especially in high-throughput settings. Cell lines such as HepG2[38] or microsomes[39] – cellular subfraction separated from the liver tissue – are easier to use but may not accurately reflect the actual liver metabolism. It has been known that the functional unit of the liver, the acinus, expresses a different set of proteins depending on the locations within the unit, and it has been speculated that it might be related to the gradient of oxygen concentration present in the liver tissue.[40] Reproducing the oxygen gradient resulted in heterogeneous distribution of P450 enzyme activity, consistent with the distribution of the actual liver.[14] Khetani *et al.* demonstrated that reproducing the co-culture pattern of primary hepatocytes and stromal cells improved various liver-specific functions.[13] Culturing rat hepatocytes in a 3-dimensional configuration and exposing the culture to fluidic flow also improved liver functions.[41,42] Mimicking the endothelial–hepatocyte interface of the liver sinusoid induced rat hepatocytes to organize into bile canaliculi along hepatic-cord like structures.[43]

It has been well demonstrated that microfabricated organ systems can improve liver functions of cultured hepatocytes, and improved liver function is likely to result in a more accurate prediction of the metabolic profile of drugs. However, adaptation into a high-throughput format is important,[44] and newly introduced systems need to be validated against *in vivo* hepatic clearance data before it can be implemented into a drug development process.

2.4 Gastrointestinal (GI) tract and absorption

Since the oral route is generally a preferred method of drug administration, and the absorption of drugs in the GI tract plays a dominant role in determining the bioavailability of the pharmacokinetic–pharmacodynamic profile of the drugs, predicting the oral drug absorption kinetics early in the drug development process is important. The *in vivo* environment of the GI tract is extremely complex, consisting of various factors. The GI tract in human male adults is several meters long, with circular tissue geometry. The lumen is separated by several layers of tissues containing mucosa, muscle, and blood vessels. The inside lining of the epithelial layer of the small intestine is covered with villi, which increase the absorptive surface area.[1] One distinctive feature of the GI tract is that it is under complex mechanical movement, including segmental contraction, peristaltic wave, and microscopic villi motility.[45] Another feature of the GI tract is that it is occupied by a large number of microbes, co-existing with intestinal epithelial cells.[46]

The two major *in vitro* methods for predicting drug absorption are the Caco-2 model[47] and the parallel artificial membrane permeability assay (PAMPA).[48] They mainly test the permeability of drugs based on passive diffusion across membranes, and neglect the other mechanisms of drug transport and complex interaction with microbiota. For example, the Caco-2 cell monolayer model was able to predict the absorption coefficient of rapidly and completely absorbed drugs, while the prediction for slowly and incompletely absorbed drugs were inaccurate.[49]

Several attempts to reproduce the microenvironment of the GI tract have been reported. Sung *et al.* developed a novel hydrogel microfabrication method to create collagen scaffold mimicking the shape of intestinal villi, and cultured Caco-2 cells into a 3-dimensional villi shape.[12] Using this 3D villi scaffold, permeability coefficients were measured and were shown to be closer to *in vivo* values than the conventional 2D model.[50] The synergistic effect of crypt topography and extracellular matrix (ECM) proteins on the Caco-2 cells was investigated by fabricating a collagen scaffold mimicking the crypt structure.[51] Kim *et al.* developed a microfluidic device for co-culturing eukaryotic HeLa cells and bacteria (*E. coli*) by compartmentalizing the device with a pneumatic valve to study the interaction of microbes and the epithelial cells.[52] Using the elastic nature of PDMS, a device operated with vacuum was developed to simulate the peristaltic movement of the GI tract.[53]

2.5 Blood-brain-barrier (BBB) and central nervous system (CNS)

The blood brain barrier (BBB) is a complex biological structure involved in the protection and maintenance of the central nervous system (CNS) against exogenous compounds present in the blood. This multi-layer structure acts as a restrictive membrane separating the blood from the cerebrospinal liquid but needs to be selectively permeable to essential compounds such as selected sugar, amino-acids, electrolytes, and water. The BBB is made primarily of three different cell types embedded in extracellular matrix which together form the neurovascular units.[54] The microvascular vessels with endothelial cells are lined by pericytes and astrocytes (glial cells). The large number of tight junctions present in the brain endothelium results in a membrane with high values of trans-endothelial electrical resistance (TEER). Moreover, most of the exchanges between the two compartments are under the control of specialized membrane transporters such as P-gycoprotein. These characteristics make the access to the brain difficult for drugs and the BBB is a major target for drug development in the pharmaceutical industry.

Currently, the replication of the BBB is performed in transmembrane-well plates. Brain microvascular endothelial cells are cultivated on the top side of the membrane while astrocytes with or without pericytes are cultivated on the bottom side.[55] Porcine, bovine, rat or murine primary cells have been used as cell sources for the BBB model, and recently human stem cells have been proposed to generate blood brain endothelial cells, astrocytes and neurons.[56] Commercially

available membranes suffer from high flow resistance due to low to modest porosity and irregular pore distribution which does not allow a close interaction between cell types. Microfabricated membranes can address these issues by reducing the global thickness and create high porosity with regular distribution of pores. Shayan *et al.* have developed a nanofabricated membrane with controlled pore size and low thickness (3 μm) allowing cell culture.[57] They demonstrated significant reduction of the flow resistance across the synthetized membrane and maintenance of metabolic activity and viability for at least three days.

Mechanical stimuli such as shear stress induced by the blood flow appear to be involved in the differentiation status of the endothelium.[58] A hollow fiber bioreactor has been developed to overcome the absence of fluid flow and shear in the standard transwell model,[59] where shear stress has been shown to induce overexpression of genes and proteins of cytoskeleton, tight-junctions and transporters. However, the interaction between the different cell types was limited by the thickness of the fiber (150 μm), and the time required to reach steady state transendothelial resistance was longer than the transwell membrane. A microfluidic based system has recently been developed to combine flow stimulation, integrated electrodes for resistance measurement and transparency for observation.[60] A porous polycarbonate membrane was sandwiched between two PDMS layers containing channels and culture chambers separating two compartments to allow dynamic culture.

Investigation of neuronal biology and CNS functionality has been limited by the lack of pertinent tools to reproduce physiologically accurate models of the neuronal microenvironment. Development of microfabricated platforms dedicated to neurobiology has opened new perspectives allowing precise spatio-temporal control of cellular environment.[61] For example, the utilization of a micropatterned surface has allowed the guidance and polarization of axonal/dendrite outgrowth in dissociated neuronal culture.[62,63] The study of the axonal biology inside a microfluidic chamber was presented by Taylor *et al.*[61] The authors developed a compartmentalized device allowing the physical separation of the neuronal body (somal side) with the axonal extension (axonal side). The platform demonstrated a significant advantage compared to the traditional methods by permitting the isolation and growth of the CNS axon, polarized through microchannels without somal and dendritic contamination. Another approach offered by this compartmentalized chamber is the possibility to co-cultivate neuron with glial cells (for example oligodendrocytes).

Multi electrode arrays or microelectrode arrays (MEA) are widely used for multi-neuron electrical recordings and have been used to model disease such as Alzheimer's disease.[64] They have been recently improved by the addition of microfluidic culture chambers and micro patterning techniques.[65] One of the limitations of the MEA system has been the difficulty of isolating the electrical signal of a single cell. By combining an MEA with replica molded PDMS channels and wells, Tinturé *et al.*[66] proposed a one-to-one electrode-neuron recording system. A promising example of this technology was applied to neurons cultivated in a dual-compartment device placed on an MEA recording system.[67] The two neuronal populations were interconnected by microchannel networks allowing the neurite extension, and recording of the electrical activity combined with a statistical connection map showed functional connection between the two populations. The use of MEA devices for *in vitro* neuronal culture systems has been recently reviewed.[68] This technology offers a significant insight in neurobiology by potentially permitting the interaction of different neuronal populations with a simultaneous recording system.

2.6 Cardiac systems

The use of perfused mammalian hearts for the study of cardiac physiology, contractile function and pathology was pioneered by Oscar Langendorff in the late 19th century.[69] The system is still currently used in functional *in vitro* studies where the effects of pathological and chemical challenges on the contractile ability of the tissue can be characterized.[70] However, its size, physiological structure and the need for intricate supporting equipment make it an impractical system for integrated chip based models. A number of systems have been developed using single cardiomyocytes to evaluate the forces generated by these cells. These systems were based on the observation of deformation of an elastic substrate,[71] pillars[72] or an attached bead;[73] or a piezoelectric force transducer.[74] However, results from a study using a small number of cardiomyocytes in an array indicated that single cells may not be suitable for testing contraction function of the heart.[75]

While single cell assays are valuable for evaluating the function of a single cell, larger microtissues of many cardiomyocytes better mimic the action of cardiomyocytes in the heart. The forces generated by sheets or films of cardiomyocytes have been measured by growing the cardiomyocytes on PDMS cantilevers,[76] PDMS films mounted on posts,[77] and PDMS films attached at one end.[78,79] The film configuration of cardiomyocytes has also been incorporated onto a diaphragm such that when the cardiomyocytes contracted, the diaphragm deformed and produced a change in pressure in the chamber.[80] Microtissues in a 3D configuration have been tested in a system of coupled vertical cantilever posts, in which a microtissue between two cantilevers bent the beams toward each other.[81] Microelectrode arrays have been used extensively for the measurement of the electrical activity of cardiomyocyte cultures and their use has been reviewed recently.[82] An extension of the system to enable patterning of the cardiomyocyte was used to evaluate drug effects on conduction velocity and the action potential refractory period in cardiomyocyte cultures.[83]

2.7 Muscle

Techniques for establishing *in vitro* cultures of primary muscle cells from both human and rodent sources have been available for over 30 years.[84] Myoblasts in culture retain the hypertrophic ability they possess *in vivo* and are therefore able to fuse, forming primary myotubes capable of functional contractile activity.[85] To date, the movement towards more biomimetic and sophisticated *in vitro* muscle models has centered on methods for improving the cellular architecture of

the various culture systems, as well as developing the means to effectively measure, characterize and maximize the functional output of the seeded cells.[86]

Three-dimensional muscle culture systems center on the use of either synthetic[87] or biopolymer[88] exogenous matrices as scaffolds in which to seed the desired cell population. In culture models utilizing 3D biopolymer matrices, cells reorganize along the lines of a principal strain, provided by cellular contraction against fixed posts, and fuse to form parallel arrays of myotubes capable of performing directed work.[89] Attachment of the culture model's fixed posts to a force transducer[89] or microscopic measurement of the matrix movement in the system[90] then allows for calculation of the specific force generated by the cells in culture. While the level of sophistication in these systems is impressive, the presence of the biopolymer matrix makes integration of other complimentary cell systems difficult.

Two dimensional culture models are far more amenable to integration into more complex body-on-a-chip type systems. Orientation of muscle cells in such models is relatively simple, relying on patterning of culture surfaces to provide the desired cellular architecture.[91,92] More problematic in these cultures is generating methods to effectively measure and quantify the functional output of the cells. The use of cantilever chips in 2D culture environments represents an elegant method for measuring the contractile activity of cultured myotubes (Fig. 1(F)).[93] When attempting to develop complex, multi-organ *in vitro* systems, such models are attractive since further patterning of these chips should allow for organized and controllable integration of other supporting cell types including Schwann cells, motoneurons and sensory neurons.

2.8 Neuromuscular junctions (NMJ)

The ability for dissociated primary muscle cells and motor neurons to generate functional neuromuscular transmission *in vitro* was first reported using chick cells by Fischbach in 1970.[94] Culture systems utilizing rodent cells were later developed and widely adopted due to the considerable advantages associated with the use of mammalian cells for studying NMJ physiology and function.[95]

The ability for primary rodent neurons and myotubes to form neuromuscular contacts *in vitro* has been demonstrated.[5] Electrophysiological recordings from such cultures suggest the existence of functional neuromuscular transmission, and spontaneous contraction of the cultured myotubes is observed and shown to be blocked by treatment with the non-depolarising neuromuscular blocker D-tubocurarine.[96] Culture systems using human and rodent derived embryonic stem cells (ESCs) with primary muscle and C2C12 muscle cell line sources have been developed.[6] These cell culture methods have the potential to be used as functional *in vitro* NMJ systems as means to test the response of novel therapeutic compounds in both healthy and diseased synapses. However, despite these advances in cell culture methods to produce and demonstrate NMJ formation, these systems have yet to be incorporated into a system suitable for use in a body-on-a-chip device.

3. Microfluidic model of whole animals

Ultimately, microfabricated organ systems can be integrated to simulate the whole-body response to drugs or pathological challenge. Although individual organ systems are not the perfect mimic of the *in vivo* tissues, such integrated model systems can be a valuable tool for studying multi-organ interactions. Interaction between two organ systems has been demonstrated by several groups[97–99] and interaction between three or four organs have also been reported,[12,100,101] but a true dynamic interaction between more than four organs has yet to be demonstrated. In this section we describe the concept of pharmacokinetics and the experimental approach to simulate multi-organ interactions *in vitro*.

3.1 Concept of pharmacokinetics

After administration, drugs go through a complex process involving absorption, distribution, metabolism and elimination (ADME). This complex process results in a time-dependent change of drug concentration in the target tissue, which affects the final pharmacological effect of drugs. The pharmacokinetics (PK) refers to the time-dependent profile of a substance in a living system.[102] While PK plays an important role in determining the pharmacological effect of a drug,[11] there is no *in vitro* system that can accurately predict the PK of drugs in humans. Currently available *in vitro* systems can recapitulate only a part of the entire process. For example, *in vitro* systems for predicting gut absorption kinetics and *in vitro* systems for predicting the liver metabolism are frequently being used in pharmaceutical research, but *in vitro* systems that can predict the dynamics of gut absorption followed by the liver metabolism have only begun to be reported in the last few years.

A mathematical modeling technique, called PK modeling, enables prediction of the drug concentration from a given dose. PK modeling is a technique widely used in pharmaceutical industry for dose optimization, and various forms of PK models exist depending on the complexity of the model. One form of a PK modeling approach, called physiologically-based pharmacokinetic (PBPK) modeling, segregates the body into organ compartments, which are connected *via* hypothetical blood flows. The mass balance for drug concentration in each compartment results in a set of ordinary differential equation that can be solved numerically.[103] Compared to other simpler forms of PK models, PBPK models provide a mechanistic basis for the model. The practical limitation of using a PBPK model for prediction of drug concentration comes from the difficulty of obtaining experimental data and finding model parameters, although various mathematical techniques to circumvent this problem exist.[104] Physical replication of PBPK models are an ideal *in vitro* platform to measure parameters, test hypotheses, and develop novel dosing strategies (Fig. 2).[10] As microfluidics allow precise control of flow and connection of multiple compartments, compartmentalized microfluidic systems can serve as an *in vitro* platform of a mathematical PBPK model.[105] The concept of using microfluidic systems as a physical representation of a PBPK model has been demonstrated.[106]

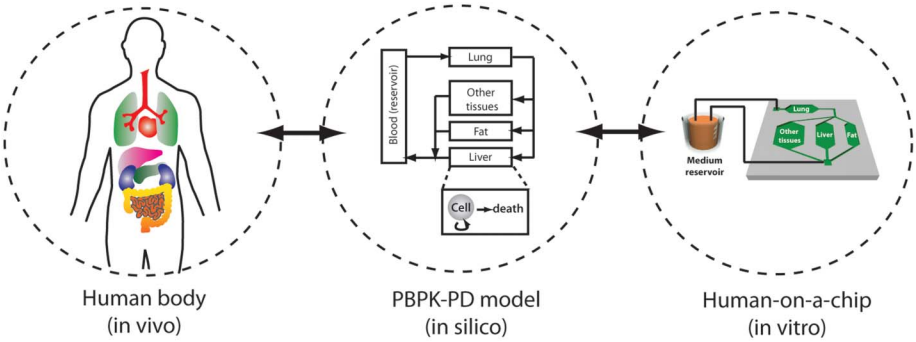

Fig. 2 Concept of physiologically-based pharmacokinetic (PBPK) model as a mathematical representation of the human body, and human-on-a-chip as a physical replication of a PBPK model.

3.2 Microfluidic systems for reproducing organ interactions

The simplest method to reproduce interactions between multiple organs is to incubate multiple cell types in a common overlying media and allow the cells to communicate *via* soluble signals. Using this concept, primary human hepatocytes and mouse fibroblasts were cultured together in a device termed integrated discrete multiple cell co-culture (IdMOC).[107] Using this device, hepatic metabolism and subsequent cytotoxicity of various compounds could be observed. However, this device lacked the time-dependent dynamics of organ interaction, as all components were submerged in a common medium, providing a homogeneous environment.

The Ahluwali group at Pisa University, Italy published a series of papers on developing a bioreactor system for reproducing multi-organ interactions.[108] Using this bioreactor system, an interaction between the hepatocytes (liver) and adipose tissue (fat) was observed.[99] By analyzing various parameters representing the liver metabolic activity, it was demonstrated that the connection of the liver and the fat compartments led to an enhancement of the liver metabolic activity. More recently the researchers extended their system to mimic a three-way interaction between the hepatocytes (liver), adipose tissue (fat), and endothelial cells (blood vessel) on glucose metabolism[100] (Fig. 3(A)). By controlling the glucose level in the perfused medium, normal and hyper-glycaemia were mimicked, and the response of each tissue model to insulin was observed by measuring the metabolites related to lipid and glucose metabolism.

Recently, several research groups have developed microfluidic systems to reproduce multi-organ interactions and the dynamics of a drug's action in the body. Van Midwoud *et al.* previously developed a novel perfusion system to incubate precision cut liver slices and observed improvement in drug metabolizing activity.[109] They extended their work to incubate a liver slice and an intestinal slice, and connected the two compartments with fluidic channels to mimic first-pass metabolism[97] (Fig. 3(B)). The interplay between the two organs was demonstrated by exposing the device to bile acid, which induced expression of fibroblast growth factor 15 in the intestinal slice and subsequent down regulation of cytochrome P450 7A1 in the liver slice.

Mao *et al.* developed a microfluidic system that reproduced liver metabolism and subsequent liver toxicity by connecting compartments containing PEG (polyethylene glycol)-encapsulated liver microsome and liver cell (HepG2) culture, and a solid-phase extraction system to purify the reaction product.[110] 5′-Diphosphate-glucuronosyltransferase (UGT) metabolism of acetaminophen and subsequent liver toxicity was characterized using this system. A device with a similar concept was reported earlier by another research group[98] (Fig. 3(C)).

In the study by Imura *et al.*, microscale models of the intestine (Caco-2 cells), the liver (HepG2 cells), and breast cancer (MCF-7 cells) were integrated to create what they termed 'micro total bioassay system'.[111] The activity of anticancer agents and estrogen-like substances were assayed using this system, and the researchers further improved the system by adding another compartment for gastrointestinal degradation prior to the intestinal absorption.[112] This compartment employed a synthetic digestive juice to reproduce the digestive process in the stomach by mixing gastric juice, drug sample and alkaline solution.

3.3 Microfluidics for reproducing the whole-body response

The concept of using a microfluidic device as a physical representation of a PBPK model was proposed by Shuler in the early 2000s. Being a physical representation of a PBPK model, the microfluidic system can serve as a physical model for reproducing whole-body response and multi-organ interactions. In 2004, Sin *et al.* reported the fabrication of a three-chamber 'microscale cell culture analog' integrated with an oxygen sensor.[113] Three chambers were fabricated on a 1 inch square silicon chip, representing the lung, liver and other tissues, and were connected by fluidic channels representing the blood flow. Although this study mainly focused on the fabrication and the operation of the device, it was the first reported example of using a microfluidic system to study multi-organ interactions. The advantage of using microfluidics was that it was possible to control the flow rate so that the fluid residence time in each chamber was set to be the residence time of corresponding organs in the human body. This kind of precise control was not achievable in previous studies that did not use microfluidics.[114] In a study using the same device, the mechanism of naphthalene toxicity was

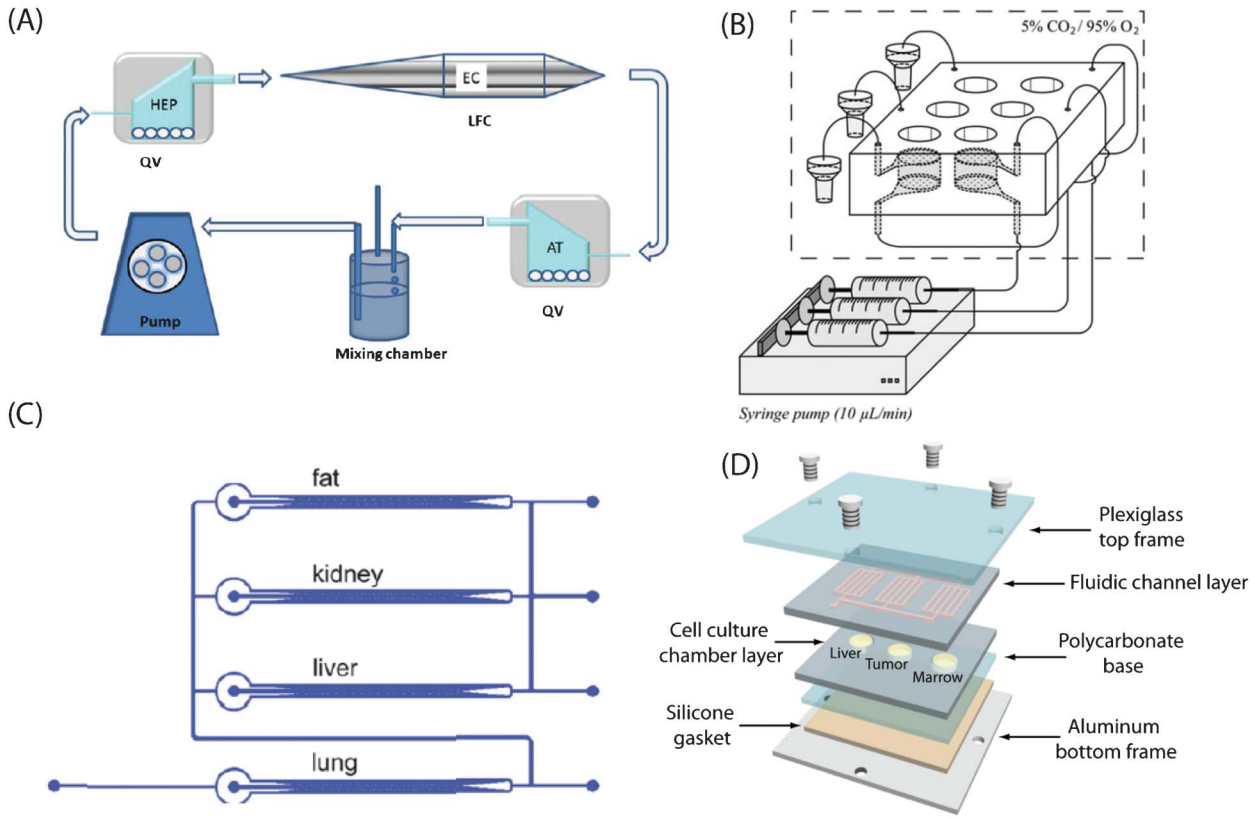

Fig. 3 (A) Schematics of 3-way connected culture, containing the hepatocytes, endothelial cells, adipose tissue. Reprinted with permission from Iori *et al.*[100] (B) Schematic of two sequentially perfused chambers (GI tract-liver). Reprinted with permission from van Midwoud *et al.*[97] (C) A multi-channel 3D microfluidic cell culture system (3D-μFCCS), containing four connected chambers on a chip. Reprinted with permission from Zhang *et al.*[118] (D) A microfluidic device for reproducing multi-organ interaction, containing three chambers connected with fluidic channels. Reprinted with permission from Sung *et al.*[106]

studied and revealed that the liver metabolism played an important role in the observed lung toxicity of naphthalene.[115] This was the first demonstration that microfluidic systems can reproduce the multi-organ interaction.

This concept was further developed to fabricate a four-chamber device to study the efficacy of drug mixtures on multidrug resistance cancers.[101] In this study, the four chambers represented the liver, bone marrow, uterine cancer, and MDR variant of uterine cancer. The liver chamber was included to simulate the liver metabolism, and the bone marrow chamber was included to simulate the toxic side effects of chemotherapeutic agents. The pharmacokinetic profile in the microfluidic device was predicted by developing a PBPK model based on the device configuration. A microfluidic module to simulate oral absorption was added to the device and acetaminophen was used to demonstrate the liver toxicity of acetaminophen after oral absorption and liver metabolism.[116] The silicon-based device was also used to incorporate 3D cell culture models to better simulate the *in vivo* tissue environment.[117] The device was further improved to better simulate the tissue environment by incorporating a cylindrical hydrogel scaffold and connecting the scaffold with fluidic channels[106] (Fig. 3(D)). This configuration was intended to mimic the tissue mass surrounded by blood vessels. Building a PBPK model based on the device and fitting the model parameters to experimental data revealed some biological insight into the mechanism of cytotoxicity.

Microfluidic systems to simulate the whole-body response have often been termed 'human-on-a-chip', or 'animal-on-a-chip'. Zhang *et al.* reported a multi-channel, 3D microfluidic cell culture system (3D-μFCCS), which contained 3D aggregates of different cells to mimic multiple organs in the body.[118] Four human cell lines were chosen to represent the liver, lung, kidney and adipose tissue. Although the researchers did not report the observation of multi-organ interaction using this device, a notable advantage of this system was the use of gelatin microspheres to selectively deliver growth factors to a specific organ (the lung in this case). This type of technique can be useful for creating organ-specific environments, while maintaining fluidic connection between the compartments. A bio-printing method was developed to seed a cell-laden hydrogel into a microfluidic device to mimic liver metabolism.[119] A similar technique was used to create a dual-tissue microfluidic chip, containing the liver cells (HepG2) and mammary epithelial cells (M10).[120] This device was used to test the effect of the radiation and radiation shielding effect of the pro-drug amifostine. Although these systems aim to reproduce interaction between multiple organs, they are mostly limited to reproducing the interaction between two organs, and the demonstration of more complex

interactions has not yet been reported. However, these preliminary systems and relevant technologies can serve as a basis to achieve more complex systems in the future.

4 Remaining challenges

Microfluidic body-on-a-chip systems have been shown to simulate parts of the human metabolism. The devices are suitable for screening new drug candidates, testing the toxicity of environmental contaminants, and conducting studies in the area of nutritional sciences. However, some challenges remain to be solved before such systems become more widely used. First, the usefulness of the devices will be enhanced if they include more organs than have been shown so far, as well as make the organ systems more functionally relevant. Currently four cell-containing chambers are the maximum number of chambers that have been included in a single chip. Incorporating more cell types into a single microchip will require more robust manipulation of fluid and cells, as well as the ability to monitor multiple cell types simultaneously. Adaptation into a high throughput format is also essential. Application of passive-mode flows such as gravity-induced flow may be a solution to achieving high throughput format.[106] Second, many of the developed systems still rely on the use of immortalized cell lines. Although these cell lines can give an estimate of tissue behavior, especially if they are human cell lines, they do not always exhibit all metabolic reactions found *in vivo*. Using primary cells, tissue samples or cells derived from stem cells will enhance the authenticity of the systems. The use of tissue samples will allow clinicians to test combinations of drugs on individual samples, thereby enabling individualized medicine for patients.

Another critical requirement for the success of multi-organ systems is the development of a blood surrogate that supports the growth of all tissues within the system. Since the cell culture media is re-circulated within the devices, all cells are exposed to the same medium components. The immobilization of growth factors within particular chambers and their controlled release could be one way to solve this problem.[118] Similarly, the removal of waste products from the medium stream will need to be accomplished. A periodic replacement of part of the volume of the recirculated medium could be a solution to the problem of waste buildup and the resulting cytotoxicity as it emulates natural processes (for example kidney) for removal of toxic metabolic byproducts. Hickman published the first serum-free, defined culture system for neuronal systems,[121] which has been applied to cardiac,[83] hippocampal neurons,[122] MNs,[123] sensory neurons,[124] muscle,[125] and NMJ formation.[6,7]

Body-on-a-chip devices will realize their full potential when bioanalytics are incorporated into the microfluidic chip. Many on-chip analytical approaches have been developed, including electrochemical electrodes, optical sensors, label-free detection of molecules, field-effect sensors, and cantilevers that sense changes in mass. These sensors are geared towards sensing small sample volumes, and sometimes include sample preparation and separation. For example, Kim and Shuler have developed an *in situ* optical detection system that can be integrated with a microfluidic device to analyze dynamics of cell viability.[126,127] This *in situ* detection and analysis system will yield more detailed information about the dynamics of multi-organ interactions. Ideally, and in order to be applied to a high-throughput format, these on-chip detection units should also be cost-effective.

5 Conclusion

An advantage that body-on-a-chip systems provide to drug toxicity testing is that metabolic reactions, even those that have not been discovered yet are incorporated within the devices *via* the cultured tissues. Comparing the data from experiments with multi-organ devices with those derived from mathematical PBPK models will allow for the verification and improvement of our understanding of specific metabolic pathways. A discrepancy will point to missing links that can be investigated further. Further, comparing data from body-on-a-chip devices that were operated with animal tissues with results obtained from animal models will validate the body-on-a-chip concept and give confidence that results from the body-on-a-chip devices with human cells would be applicable to humans prior to testing on humans. For this purpose, a combination of mathematical and experimental approaches is essential for the effective study of the dynamics of multi-organ interaction. We believe that such devices will assume an increasingly important role in pharmaceutical and medical sciences.

Acknowledgements

JHS gratefully acknowledges support from National Research Foundation of Korea (NRF, Grant No. 2012-0003408), KFRI (Korea Food Research Institute, grant No: E0121705), 2012 Hongik University Research Fund. James Hickman's work is funded under NIH grant numbers R01NS050452 and R01EB009429

References

1 P. Artursson, K. Palm and K. Luthman, *Adv. Drug Delivery Rev.*, 2001, **46**, 27–43.
2 A. Abbott, *Nature*, 2003, **424**, 870–872.
3 A. L. Paguirigan and D. J. Beebe, *BioEssays*, 2008, **30**, 811–821.
4 A. Khademhosseini and R. Langer, *Biomaterials*, 2007, **28**, 5087–5092.
5 M. Das, J. W. Rumsey, N. Bhargava, M. Stancescu and J. J. Hickman, *Biomaterials*, 2010, **31**, 4880–4888.
6 X. Guo, M. Gonzalez, M. Stancescu, H. H. Vandenburgh and J. J. Hickman, *Biomaterials*, 2011, **32**, 9602–9611.
7 X. Guo, M. Das, J. Rumsey, M. Gonzalez, M. Stancescu and J. Hickman, *Tissue Eng., Part C*, 2010, **16**, 1347–1355.

8 J. El-Ali, P. K. Sorger and K. F. Jensen, *Nature*, 2006, **442**, 403–411.
9 M. B. Esch, J. H. Sung and M. L. Shuler, *J. Biotechnol.*, 2010, **148**, 64–69.
10 J. H. Sung, M. B. Esch and M. L. Shuler, *Expert Opin. Drug Metab. Toxicol.*, 2010, **6**, 1063–1081.
11 I. Kola and J. Landis, *Nat. Rev. Drug Discovery*, 2004, **3**, 711–715.
12 J. H. Sung, J. Yu, D. Luo, M. L. Shuler and J. C. March, *Lab Chip*, 2011, **11**, 389–392.
13 S. R. Khetani and S. N. Bhatia, *Nat. Biotechnol.*, 2008, **26**, 120–126.
14 J. W. Allen, S. R. Khetani and S. N. Bhatia, *Toxicol. Sci.*, 2005, **84**, 110–119.
15 D. Huh, B. D. Matthews, A. Mammoto, M. Montoya-Zavala, H. Y. Hsin and D. E. Ingber, *Science*, 2010, **328**, 1662–1668.
16 A. Ajdari, *C. R. Phys.*, 2003, **5**, 539–546.
17 K. W. Oh, K. Lee, B. Ahn and E. P. Furlani, *Lab Chip*, 2012, **12**, 515–545.
18 E. W. Young, A. R. Wheeler and C. A. Simmons, *Lab Chip*, 2007, **7**, 1759–1766.
19 E. Gutierrez and A. Groisman, *Anal. Chem.*, 2007, **79**, 2249–2258.
20 A. D. van der Meer, K. Vermeul, A. A. Poot, J. Feijen and I. Vermes, *Am. J. Physiol.: Heart Circ. Physiol.*, 2010, **298**, H719–725.
21 Y. Shin, J. S. Jeon, S. Han, G. S. Jung, S. Shin, S. H. Lee, R. Sudo, R. D. Kamm and S. Chung, *Lab Chip*, 2011, **11**, 2175–2181.
22 E. Berthier, E. W. Young and D. Beebe, *Lab Chip*, 2012, **12**, 1224–1237.
23 M. C. Cushing and K. S. Anseth, *Science*, 2007, **316**, 1133–1134.
24 T. Frisk, S. Rydholm, H. Andersson, G. Stemme and H. Brismar, *Electrophoresis*, 2005, **26**, 4751–4758.
25 N. W. Choi, M. Cabodi, B. Held, J. P. Gleghorn, L. J. Bonassar and A. D. Stroock, *Nat. Mater.*, 2007, **6**, 908–915.
26 Y. Zheng, J. Chen, M. Craven, N. W. Choi, S. Totorica, A. Diaz-Santana, P. Kermani, B. Hempstead, C. Fischbach-Teschl, J. A. Lopez and A. D. Stroock, *Proc. Natl. Acad. Sci. U. S. A.*, 2012, **109**, 9342–9347.
27 M. P. Cuchiara, A. C. Allen, T. M. Chen, J. S. Miller and J. L. West, *Biomaterials*, 2010, **31**, 5491–5497.
28 A. P. Golden and J. Tien, *Lab Chip*, 2007, **7**, 720–725.
29 L. M. Bellan, S. P. Singh, P. W. Henderson, T. J. Porri, H. G. Craighead and J. A. Spector, *Soft Matter*, 2009, **5**, 1354–1357.
30 A. Tam, S. Wadsworth, D. Dorscheid, S. F. Man and D. D. Sin, *Ther. Adv. Respir. Dis.*, 2011, **5**, 255–273.
31 D. D. Nalayanda, C. Puleo, W. B. Fulton, L. M. Sharpe, T. H. Wang and F. Abdullah, *Biomed. Microdevices*, 2009.
32 D. Huh, H. Fujioka, Y. C. Tung, N. Futai, R. Paine, 3rd, J. B. Grotberg and S. Takayama, *Proc. Natl. Acad. Sci. U. S. A.*, 2007, **104**, 18886–18891.
33 N. J. Douville, Y. C. Tung, R. Li, J. D. Wang, M. E. El-Sayed and S. Takayama, *Anal. Chem.*, 2010, **82**, 2505–2511.
34 C. Long, C. Finch, M. Esch, W. Anderson, M. Shuler and J. Hickman, *Ann. Biomed. Eng.*, 2012, **40**, 1255–1267.
35 E. F. Brandon, C. D. Raap, I. Meijerman, J. H. Beijnen and J. H. Schellens, *Toxicol. Appl. Pharmacol.*, 2003, **189**, 233–246.
36 S. Ekins, *Drug Metab. Rev.*, 1996, **28**, 591–623.
37 D. M. Cross and M. K. Bayliss, *Drug Metab. Rev.*, 2000, **32**, 219–240.
38 W. M. Westerink and W. G. Schoonen, *Toxicol. in Vitro*, 2007, **21**, 1581–1591.
39 C. Lu, P. Li, R. Gallegos, V. Uttamsingh, C. Q. Xia, G. T. Miwa, S. K. Balani and L. S. Gan, *Drug Metab. Dispos.*, 2006, **34**, 1600–1605.
40 J. P. Camp and A. T. Capitano, *Biotechnol. Prog.*, 2007, **23**, 1485–1491.
41 K. Domansky, W. Inman, J. Serdy, A. Dash, M. H. Lim and L. G. Griffith, *Lab Chip*, 2010, **10**, 51–58.
42 A. Sivaraman, J. K. Leach, S. Townsend, T. Iida, B. J. Hogan, D. B. Stolz, R. Fry, L. D. Samson, S. R. Tannenbaum and L. G. Griffith, *Curr. Drug Metab.*, 2005, **6**, 569–591.
43 Y. Nakao, H. Kimura, Y. Sakai and T. Fujii, *Biomicrofluidics*, 2011, **5**, 22212.
44 M. Y. Lee and J. S. Dordick, *Curr. Opin. Biotechnol.*, 2006, **17**, 619–627.
45 C. P. Gayer and M. D. Basson, *Cell. Signalling*, 2009, **21**, 1237–1244.
46 M. B. Clarke and V. Sperandio, *Am. J.Physiol.: Gastrointest. Liver Physiol.*, 2005, **288**, G1105–1109.
47 I. Hubatsch, E. G. Ragnarsson and P. Artursson, *Nat. Protoc.*, 2007, **2**, 2111–2119.
48 J. M. Reis, B. Sinko and C. H. Serra, *Mini-Rev. Med. Chem.*, 2010, **10**, 1071–1076.
49 C. L. Stevenson, P. F. Augustijns and R. W. Hendren, *Int. J. Pharm.*, 1999, **177**, 103–115.
50 J. Yu, S. Peng, D. Luo and J. C. March, *Biotechnol. Bioeng.*, 2012.
51 L. Wang, S. K. Murthy, G. A. Barabino and R. L. Carrier, *Biomaterials*, 2010, **31**, 7586–7598.
52 J. Kim, M. Hegde and A. Jayaraman, *Lab Chip*, 2010, **10**, 43–50.
53 H. J. Kim, D. Huh, G. Hamilton and D. E. Ingber, *Lab Chip*, 2012, **12**, 2165–2174.
54 B. T. Hawkins and T. P. Davis, *Pharmacol. Rev.*, 2005, **57**, 173–185.
55 K. Hatherell, P. O. Couraud, I. A. Romero, B. Weksler and G. J. Pilkington, *J. Neurosci. Methods*, 2011, **199**, 223–229.
56 E. S. Lippmann, S. M. Azarin, J. E. Kay, R. A. Nessler, H. K. Wilson, A. Al-Ahmad, S. P. Palecek and E. V. Shusta, *Nat. Biotechnol.*, 2012.
57 G. Shayan, N. Felix, Y. Cho, M. Chatzichristidi, M. L. Shuler, C. K. Ober and K. H. Lee, *Tissue Eng., Part C*, 2012.
58 L. Cucullo, M. Hossain, V. Puvenna, N. Marchi and D. Janigro, *BMC Neurosci.*, 2011, **12**, 40.
59 D. Janigro, S. M. Leaman and K. A. Stanness, *Pharm. Sci. Technol. Today*, 1999, **2**, 7–12.
60 R. Booth and H. Kim, *Lab Chip*, 2012, **12**, 1784–1792.
61 A. M. Taylor and N. L. Jeon, *Curr. Opin. Neurobiol.*, 2010, **20**, 640–647.
62 D. A. Stenger, J. J. Hickman, K. E. Bateman, M. S. Ravenscroft, W. Ma, J. J. Pancrazio, K. Shaffer, A.

E. Schaffner, D. H. Cribbs and C. W. Cotman, *J. Neurosci. Methods*, 1998, **82**, 167–173.
63 P. Molnar, N. Bhargava, M. Das and J. J. Hickman, in *Methods in Molecular Biology*, ed. P. Molnar and J. J. Hickman, Humana Press, New York, 2007.
64 K. Varghese, P. Molnar, M. Das, N. Bhargava, S. Lambert, M. S. Kindy and J. J. Hickman, *PLoS One*, 2010, **5**, e8643.
65 F. Morin, N. Nishimura, L. Griscom, B. Lepioufle, H. Fujita, Y. Takamura and E. Tamiya, *Biosens. Bioelectron.*, 2006, **21**, 1093–1100.
66 E. Claverol-Tinturé, X. Rosell and J. Cabestany, *Neurocomputing*, 2007, **70**, 2716–2722.
67 T. T. Kanagasabapathi, D. Ciliberti, S. Martinoia, W. J. Wadman and M. M. Decre, *Front. Neuroeng.*, 2011, **4**, 13.
68 A. F. Johnstone, G. W. Gross, D. G. Weiss, O. H. Schroeder, A. Gramowski and T. J. Shafer, *NeuroToxicology*, 2010, **31**, 331–350.
69 O. Langendorff, *Pfluegers Arch.*, 1895, **61**, 291–332.
70 R. M. Bell, M. M. Mocanu and D. M. Yellon, *J. Mol. Cell. Cardiol.*, 2011, **50**, 940–950.
71 J. G. Jacot, A. D. McCulloch and J. H. Omens, *Biophys. J.*, 2008, **95**, 3479–3487.
72 Y. Tanaka, K. Morishima, T. Shimizu, A. Kikuchi, M. Yamato, T. Okano and T. Kitamori, *Lab Chip*, 2006, **6**, 230–235.
73 S. Yin, X. Zhang, C. Zhan, J. Wu, J. Xu and J. Cheung, *Biophys. J.*, 2005, **88**, 1489–1495.
74 G. Lin, R. E. Palmer, K. S. Pister and K. P. Roos, *IEEE Trans. Biomed. Eng.*, 2001, **48**, 996–1006.
75 T. Kaneko, K. Kojima and K. Yasuda, *Analyst*, 2007, **132**, 892–898.
76 J. Kim, J. Park, K. Na, S. Yang, J. Baek, E. Yoon, S. Choi, S. Lee, K. Chun and S. Park, *J. Biomech.*, 2008, **41**, 2396–2401.
77 P. W. Alford, A. W. Feinberg, S. P. Sheehy and K. K. Parker, *Biomaterials*, 2010, **31**, 3613–3621.
78 A. Grosberg, A. P. Nesmith, J. A. Goss, M. D. Brigham, M. L. McCain and K. K. Parker, *J. Pharmacol. Toxicol. Methods*, 2012, **65**, 126–135.
79 A. Grosberg, P. W. Alford, M. L. McCain and K. K. Parker, *Lab Chip*, 2011, **11**, 4165–4173.
80 P. Linder, J. Trzewik, M. Ruffer, G. M. Artmann, I. Digel, R. Kurz, A. Rothermel, A. Robitzki and A. Temiz Artmann, *Med. Biol. Eng. Comput.*, 2010, **48**, 59–65.
81 T. Boudou, W. R. Legant, A. Mu, M. A. Borochin, N. Thavandiran, M. Radisic, P. W. Zandstra, J. A. Epstein, K. B. Margulies and C. S. Chen, *Tissue Eng. A*, 2012, **18**, 910–919.
82 I. L. Jones, P. Livi, M. K. Lewandowska, M. Fiscella, B. Roscic and A. Hierlemann, *Anal. Bioanal. Chem.*, 2011, **399**, 2313–2329.
83 A. Natarajan, M. Stancescu, V. Dhir, C. Armstrong, F. Sommerhage, J. J. Hickman and P. Molnar, *Biomaterials*, 2011, **32**, 4267–4274.
84 R. Bischoff, *Anat. Rec.*, 1974, **180**, 645–661.
85 H. Vandenburgh, *Tissue Eng., Part B: Rev.*, 2010, **16**, 55–64.
86 K. Wilson, M. Das, K. J. Wahl, R. J. Colton and J. Hickman, *PLoS One*, 2010, **5**, e11042.
87 S. Levenberg, J. Rouwkema, M. Macdonald, E. S. Garfein, D. S. Kohane, D. C. Darland, R. Marini, C. A. van Blitterswijk, R. C. Mulligan, P. A. D'Amore and R. Langer, *Nat. Biotechnol.*, 2005, **23**, 879–884.
88 S. Hinds, W. Bian, R. G. Dennis and N. Bursac, *Biomaterials*, 2011, **32**, 3575–3583.
89 A. Khodabukus and K. Baar, *Tissue Eng., Part C*, 2012, **18**, 349–357.
90 H. Vandenburgh, J. Shansky, F. Benesch-Lee, V. Barbata, J. Reid, L. Thorrez, R. Valentini and G. Crawford, *Muscle Nerve*, 2008, **37**, 438–447.
91 N. F. Huang, S. Patel, R. G. Thakar, J. Wu, B. S. Hsiao, B. Chu, R. J. Lee and S. Li, *Nano Lett.*, 2006, **6**, 537–542.
92 P. Molnar, W. Wang, A. Natarajan, J. W. Rumsey and J. J. Hickman, *Biotechnol. Prog.*, 2007, **23**, 265–268.
93 M. Das, K. Wilson, P. Molnar and J. J. Hickman, *Nat. Protoc.*, 2007, **2**, 1795–1801.
94 G. D. Fischbach, *Science*, 1970, **169**, 1331–1333.
95 M. P. Daniels, B. T. Lowe, S. Shah, J. Ma, S. J. Samuelsson, B. Lugo, T. Parakh and C. S. Uhm, *Microsc. Res. Tech.*, 2000, **49**, 26–37.
96 M. Das, J. W. Rumsey, C. A. Gregory, N. Bhargava, J. F. Kang, P. Molnar, L. Riedel, X. Guo and J. J. Hickman, *Neuroscience*, 2007, **146**, 481–488.
97 P. M. van Midwoud, M. T. Merema, E. Verpoorte and G. M. Groothuis, *Lab Chip*, 2010, **10**, 2778–2786.
98 B. Ma, G. Zhang, J. Qin and B. Lin, *Lab Chip*, 2009, **9**, 232–238.
99 M. A. Guzzardi, C. Domenici and A. Ahluwalia, *Tissue Eng. A*, 2011, **17**, 1635–1642.
100 E. Iori, B. Vinci, E. Murphy, M. C. Marescotti, A. Avogaro and A. Ahluwalia, *PLoS One*, 2012, **7**, e34704.
101 D. A. Tatosian and M. L. Shuler, *Biotechnol. Bioeng.*, 2009, **103**, 187–198.
102 L. E. Gerlowski and R. K. Jain, *J. Pharm. Sci.*, 1983, **72**, 1103–1127.
103 J. H. Sung, A. Dhiman and M. L. Shuler, *J. Pharm. Sci.*, 2009, **98**, 1885–1904.
104 L. Aarons, *Br. J. Clin. Pharmacol.*, 2005, **60**, 581–583.
105 C. Moraes, G. Mehta, S. C. Lesher-Perez and S. Takayama, *Ann. Biomed. Eng.*, 2012, **40**, 1211–1227.
106 J. H. Sung, C. Kam and M. L. Shuler, *Lab Chip*, 2010, **10**, 446–455.
107 A. P. Li, A. Uzgare and Y. S. Laforge, *Chem.-Biol. Interact.*, 2012, **199**, 1–8.
108 F. Vozzi, D. Mazzei, B. Vinci, G. Vozzi, T. Sbrana, L. Ricotti, N. Forgione and A. Ahluwalia, *Biotechnol. Bioeng.*, 2011, **108**, 2129–2140.
109 P. M. van Midwoud, G. M. Groothuis, M. T. Merema and E. Verpoorte, *Biotechnol. Bioeng.*, 2010, **105**, 184–194.
110 S. Mao, D. Gao, W. Liu, H. Wei and J. M. Lin, *Lab Chip*, 2012, **12**, 219–226.
111 Y. Imura, K. Sato and E. Yoshimura, *Anal. Chem.*, 2010, **82**, 9983–9988.
112 Y. Imura, E. Yoshimura and K. Sato, *Anal. Sci.*, 2012, **28**, 197–199.
113 A. Sin, K. C. Chin, M. F. Jamil, Y. Kostov, G. Rao and M. L. Shuler, *Biotechnol. Prog.*, 2004, **20**, 338–345.
114 A. Ghanem and M. L. Shuler, *Biotechnol. Prog.*, 2000, **16**, 471–479.
115 K. Viravaidya, A. Sin and M. L. Shuler, *Biotechnol. Prog.*, 2004, **20**, 316–323.

116 G. J. Mahler, M. B. Esch, R. P. Glahn and M. L. Shuler, *Biotechnol. Bioeng.*, 2009, **104**, 193–205.
117 J. H. Sung and M. L. Shuler, *Lab Chip*, 2009, **9**, 1385–1394.
118 C. Zhang, Z. Zhao, N. A. Abdul Rahim, D. van Noort and H. Yu, *Lab Chip*, 2009, **9**, 3185–3192.
119 R. Chang, K. Emami, H. Wu and W. Sun, *Biofabrication*, 2010, **2**, 045004.
120 J. E. Snyder, Q. Hamid, C. Wang, R. Chang, K. Emami, H. Wu and W. Sun, *Biofabrication*, 2011, **3**, 034112.
121 A. E. Schaffner, J. L. Barker, D. A. Stenger and J. J. Hickman, *J. Neurosci. Methods*, 1995, **62**, 111–119.
122 K. Varghese, M. Das, N. Bhargava, M. Stancescu, P. Molnar, M. S. Kindy and J. J. Hickman, *J. Neurosci. Methods*, 2009, **177**, 51–59.
123 M. Das, P. Molnar, H. Devaraj, M. Poeta and J. J. Hickman, *Biotechnol. Prog.*, 2003, **19**, 1756–1761.
124 J. W. Rumsey, M. Das, A. Bhalkikar, M. Stancescu and J. J. Hickman, *Biomaterials*, 2010, **31**, 8218–8227.
125 M. Das, C. A. Gregory, P. Molnar, L. M. Riedel, K. Wilson and J. J. Hickman, *Biomaterials*, 2006, **27**, 4374–4380.
126 J. R. Choi, J. H. Sung, M. L. Shuler and D. Kim, *Opt. Lett.*, 2010, **35**, 1374–1376.
127 J. H. Sung, J. R. Choi, D. Kim and M. L. Shuler, *Biotechnol. Bioeng.*, 2009, **104**, 516–525.

